The Sixteenth International Congress on Sound and Vibration
Kraków, 5-9 July 2009

MODELLING MULTI-MODAL SOUND TRANSMISSION FROM POINT SOURCES IN DUCTS WITH FLOW USING A WAVE-BASED METHOD

Gareth J. Bennett, Ciarán J. O'Reilly, Hao Liu

Dept. of Mechanical and Manufacturing Engineering, Trinity College, Dublin 2, Ireland.
email: gareth.bennett@tcd.ie

Ulf Tapken

German Aerospace Center (DLR),
Institute of Propulsion Technology, Engine Acoustics Branch,
Muller-Breslau-Str. 8, 10623 Berlin, Germany.

An understanding of the multi-modal propagation of acoustic waves in ducts is of practical interest for use in the control of noise in, for example, aero-engines, automotive exhaust and ventilation systems. In this paper, the propagation of sound from point sources in hard-walled ducts is modelled using a numerical wave-based approach, referred to as the wave expansion method. This is a highly efficient full-domain discretisation method, which requires as few as two-to-three mesh points per wavelength. An inhomogeneous potential flow may be easily included in the method. The numerical solution for point sources embedded in the wall of a circular duct with non-reflective end-conditions and a uniform axial flow is compared with an analytical Green's function solution. A modal decomposition technique is used to provide detailed information about the modal content of the sound field. This study provides an insightful comparison between an analytical and numerical solution to the acoustic field in a duct. The accuracy and robustness of the wave expansion method is assessed for this benchmark problem before its versatility is demonstrated with examples.

1. Introduction

The Wave Expansion Method, originally introduced by Caruthers [1], has received much attention due to the fact that it is a highly efficient numerical procedure. Many applications have been examined, its efficiency being of particular interest to large-scale sound propagation problems [2]. In this paper its applicability to duct acoustics is examined. The fact that it can be adapted to complex duct geometries and flow fields could be of great interest in the study of sound propagation in aero-engines. A preliminary investigation as to its appropriateness is presented here. For a simple duct geometry, the numerical calculation is compared to the exact analytical solution based on a Green's function distribution of single and multiple volume sources. The acoustic pressure field is examined visually and by performing a modal decomposition greater insight into the acoustic structures is obtained. In order to demonstrate the advantages of the WEM technique over the analytical solution, some additional calculations are performed.

2. Description of Mode Propagation in Hard Walled Cylindrical Flow Ducts

For acoustic propagation in an infinite hard walled cylindrical duct with superimposed constant mean flow velocity **U**, the pressure $p = p(r, \theta, x, t)$, in cylindrical coordinates, is found as a solution of the homogeneous convective wave equation,

$$\frac{1}{c^2}\frac{\mathrm{D}^2 p}{\mathrm{D}t^2} - \frac{\partial^2 p}{\partial x^2} - \frac{1}{r}\frac{\partial}{\partial r}\left(r\frac{\partial p}{\partial r}\right) - \frac{1}{r^2}\frac{\partial^2 p}{\partial \theta^2} = 0 \tag{1}$$

where the substantive derivative is defined to be

$$\frac{\mathrm{D}}{\mathrm{D}t} = \frac{\partial}{\partial t} + \mathbf{U}.\nabla$$

This solution is found as a combination of the characteristic functions of equation (1) each of which satisfy specific boundary conditions. Rigorous treatments of the derivation of the separation-of-variables solution can be found in the literature [3, 4, 5] . For the following assumptions that;

- The flow is incompressible and isentropic with negligible temperature gradients
- The mean flow speed, $\mathbf{U} = (U_x, 0, 0)$ is stationary with time
- The axial mean flow profile as well as the duct cross-sectional area are invariant in the axial direction
- The mean temperature and the density are stationary in space and time

the solution to the wave equation for the complex pressure can be given by a linear superposition of modal terms:

$$\hat{p}(x, r, \varphi) = \sum_{m=-\infty}^{\infty}\sum_{n=0}^{\infty}\left[A^+_{m,n} e^{(-jk^+_{m,n}x)} + A^-_{m,n} e^{(+jk^-_{m,n}x)}\right] f_{m,n}(r) e^{(jm\varphi)} \tag{2}$$

where $A^+_{m,n}$ and $A^-_{m,n}$ are the complex amplitudes of the modes, $k^+_{m,n}x$ and $k^-_{m,n}x$ are the axial wave numbers, and m and n are the azimuthal and radial mode indices respectively. The $+$ superscript refers to the direction of flow whereas the $-$ superscript indicates the parameter to be defined counter to the flow direction. In the case of hard-walled acoustic boundary conditions, the modes form an orthogonal eigensystem, with a modal shape factor given by

$$f_{m,n}(r) = \frac{\mathrm{J}_m\left(\sigma_{mn} r/R\right)}{\sqrt{N_{m,n}}} \tag{3}$$

for a non-annular cylinder. In equation (3), J_m is a Bessel function of the first kind of order m with associated hard-walled cylindrical eigenvalue σ_{mn}. R is the duct outer radius and in order to satisfy orthogonality the normalisation factor is calculated to be

$$N_{mn} = 2\pi\int_0^R \mathrm{J}^2_m\left(\sigma_{mn} r/R\right) r\, dr = \pi R^2\left(\mathrm{J}^2_m\left(\sigma_{mn}\right) - \mathrm{J}_{m-1}\left(\sigma_{mn}\right)\mathrm{J}_{m+1}\left(\sigma_{mn}\right)\right) \tag{4}$$

The normalisation transforms the orthogonal mode eigensystem into an orthonormal mode eigensystem. A mean flow can be accommodated in the formulation by modification of the axial wave numbers which are a function of the mode eigenvalue σ_{mn} and the free field propagation wave number, k, which are defined as follows

$$k^{\pm}_{mn} = k\,\frac{-M_x \pm \alpha_{mn}}{\beta^2} \qquad where \qquad \alpha_{mn} = \sqrt{1 - \left(\frac{\beta\sigma_{mn}}{kR}\right)^2} \qquad and \qquad \beta = \sqrt{1 - M_x^2} \tag{5}$$

3. Wave Expansion Method

If the mean flow is assumed to be irrotational and inhomogeneous then it can be modelled as a potential flow, and the governing field equation for the velocity potential, ϕ is given by

$$\frac{1}{\rho}\nabla.\left(\rho\,\nabla\phi\right) - L\left(\frac{1}{c^2}L\phi\right) = 0 \tag{6}$$

where L is the complex linear operator $(i\omega + \mathbf{U}.\nabla)$ and $\mathbf{U}$, ρ, c, are the local mean velocity, density, and speed of sound respectively. The acoustic parts of the velocity potential and pressure are related by

$$\hat{p} = -\rho j\omega\phi - \rho\mathbf{U}.\nabla\phi \tag{7}$$

The velocity potential at a discrete point, $\phi_{\mathbf{0}}$, (the subscript '0' denotes the value at the point in question) may be computed from the amplitude and phase of M neighbouring points. The potential at each point in a domain may be approximated by the superposition of the field generated by N hypothetical plane waves of strength γ_n and with unit propagation in direction $\mathbf{d}_n$ such that

$$\phi_{\mathbf{0}} = \sum_{n=1}^{N}\gamma_n \exp\left[-iq\left(\mathbf{d}.\mathbf{x_0}\right)\right] = \mathbf{h}\boldsymbol{\gamma} \tag{8}$$

where $h_n = \exp\left[-iq\left(\mathbf{d}.\mathbf{x_0}\right)\right]$,

$$q = \frac{i\mathbf{B_0}.\mathbf{d} \pm \sqrt{4K_{\mathbf{0}}^2\left(1 - \left(\mathbf{M_0}.\mathbf{d}\right)^2\right) - \left(\mathbf{B_0}.\mathbf{d}\right)^2}}{2\left(1 - \left(\mathbf{M_0}.\mathbf{d}\right)^2\right)} \tag{9}$$

where

$$\mathbf{B} = 2ik\mathbf{M} + \mathbf{U}.\nabla\left(\frac{1}{c^2}\right)\mathbf{U} + \frac{1}{c^2}\mathbf{U}.\nabla\,\mathbf{U} - \frac{1}{\rho}\nabla\,\rho \tag{10}$$

$$K^2 = \frac{\omega^2}{c^2} - i\omega\,\mathbf{U}.\nabla\frac{1}{c^2} \tag{11}$$

and where $\mathbf{M} = \mathbf{U}/c$. Similarly, the velocity potential at a neighbouring point, $\mathbf{m}$, in the computational lattice, where $\mathbf{m} = 1, 2, .., M$, is given as

$$\boldsymbol{\phi}_{\mathbf{m}} = \sum_{n=1}^{N}\gamma_n \exp\left[-iq\left(\mathbf{d}.\mathbf{x_m}\right)\right] = \mathbf{H}\boldsymbol{\gamma} \tag{12}$$

If $\mathbf{H}^+$ is the pseudo-inverse of $\mathbf{H}$ then

$$\boldsymbol{\gamma} = \mathbf{H}^+\boldsymbol{\phi}_{\mathbf{m}}\,, \tag{13}$$

and substituting this back into equation (8) leads to

$$\phi_{\mathbf{0}} - \mathbf{h}\mathbf{H}^+\boldsymbol{\phi}_{\mathbf{m}} = 0\,. \tag{14}$$

If the he local stiffness vector for a computational lattice is $\kappa_{\mathbf{0}} = -\mathbf{h}\mathbf{H}^+$, then

$$\phi_{\mathbf{0}} + \kappa_{\mathbf{0}}\boldsymbol{\phi}_{\mathbf{m}} = 0\,, \tag{15}$$

which may be rewritten as

$$\left\{ \begin{array}{cc} 1 & \kappa_{\mathbf{0}} \end{array} \right\} \left\{ \begin{array}{c} \phi_{\mathbf{0}} \\ \boldsymbol{\phi}_{\mathbf{m}} \end{array} \right\} = 0\,. \tag{16}$$

For the total computational domain, with a source vector, $\mathbf{f}$, added to the right-hand-side and where $\boldsymbol{\kappa}$ is the overall stiffness matrix, a linear system of equations may be defined of the form

$$\boldsymbol{\kappa\phi} = \mathbf{f}\,. \tag{17}$$

This may, with the addition of appropriate boundary conditions (see [6]), be solved for $\boldsymbol{\phi}$, a vector containing the velocity potential at each point in the overall computational lattice.

4. Analytical Solution in Terms of Point Source Distribution

In order to have a benchmark case against which the Wave Based Method could be compared, results from an exact analytical solution were generated. The frequency-domain Green's function for a duct with an axial irrotational mean flow must satisfy

$$\left(\nabla^2 - M_x^2 \frac{\partial^2}{\partial x^2} - 2ikM_x \frac{\partial}{\partial x} + k^2\right) \mathrm{G}\left(\mathbf{x}, \mathbf{y}\right) = -\delta\left(\mathbf{x} - \mathbf{y}\right) \tag{18}$$

and for a hard-walled boundary condition

$$\frac{\partial \mathrm{G}}{\partial \mathbf{n}} = 0 \tag{19}$$

where **n** is a unit vector normal to the surface of the duct.

Following the formulation of Goldstein [7], the sound pressure generated at position (x, r, φ) due to a single monopole source with volume velocity $q_0 = v_0 A$ located at $(x_{q0}, r_{q0}, \varphi_{q0})$ can be expressed as

$$p^{(\leftrightarrows)}(x, r, \varphi | x_{q0}, r_{q0}, \varphi_{q0}) = -j\omega\rho q_0 g^{(\leftrightarrows)}(x, r, \varphi | x_{q0}, r_{q0}, \varphi_{q0}) \tag{20}$$

$$= q_0 \frac{\rho c}{2} \sum_{m=-\infty}^{\infty} \sum_{n=0}^{\infty} \frac{\mathrm{J}_m\left(\sigma_{mn} r/R\right) \mathrm{J}_m\left(\sigma_{mn} r_{q_0}/R\right)}{\alpha_{mn} N_{mn}}\, \mathrm{e}^{-im\left(\phi - \phi_{q_0}\right)}\, \mathrm{e}^{-ik_{mn}^{\pm}\left(x - x_{q_0}\right)} \tag{21}$$

where q_0 is the source volume velocity, ρ and c are the density and speed of sound of the propagation medium.

Whereas a single monopole source will excite all modes, specific modes can be excited by locating multiple sources around the duct and by adjusting their phases appropriately using the expressions of equation 22. The total sound field is found through superposition of equation 21 for each source.

$$q(\theta_l) = q_m e^{\left(im\frac{2\pi l}{S}\right)} \qquad where \qquad \left| \begin{array}{l} l = 0, 1, \ldots, (S-1); \\ \theta_l = \dfrac{2\pi l}{S} \end{array} \right. \tag{22}$$

5. Results and Analysis

The first means of comparison between the analytical solution and the Wave Expansion Method was the pressure field generated in the duct due to a single monopole located on the interior duct surface. As mentioned, a single monopole source will excite all modes and figure 1 presents the results for a comparison between the analytical solution and those from the WEM for a Helmholtz number of 5.9. The agreement is seen to be very good both on the wall surface and within the volume of the duct.

Some investigation of the sensitivity of the results as a function of mesh density for the WEM was carried out, the results of which can be seen in figure 2. The theoretical and numerical results for the transfer function for a mesh nodal spacing of $0.26m$ is shown in figure 2(a). Using a two microphone technique such as that of Chung and Blaser's [8], the reflection coefficient for the plane wave frequency range can be calculated, results of which are shown in figure 2(b). As can be seen, the results are improved upon by increasing the number of points per wavelength, however, if the density is too great the low frequency results disimprove. This is due to ill-conditioning in the system matrices. Thus, an optimum density must be employed for the frequency range of interest.

The next comparison was performed with eight monopole sources to excite a specific azimuthal mode, in this case $A_m = A_1$. Figures 3 and 4 show the comparison between the pressure fields for two Helmholtz numbers, the higher one being above the cut-on frequency of the first radial mode. Again the comparison is excellent although being 180 degrees out of phase with each other presumably due to a phase shift in the monopole phases between the two cases.

The model's capability to incorporate a mean flow is demonstrated in figure 5. In both cases, which agree closely, the wavelengths are modified upstream and downstream of the monopole source.

5.1 Acoustic Modal Decomposition in Hard Walled Cylindrical Flow Ducts

The gain some deeper insight into the pressure field comparisons, a modal decomposition was performed using both sets of data. The method employed in this paper is based on the approach proposed by Åbom [9] and further details can be found in Bennett [10, 11], where this technique was implemented with both experimental and numerical data. Similar to the techniques described by Enghardt *et al.* [12] and Tapken and Enghardt [13], the procedure uses an array of axially and azimuthally distributed wall surface location measurements, and consists of solving equation (2) for the modal amplitudes, $A^{\pm}_{m,n}$. The configuration for the "microphone" arrays are four axial locations separated by $0.05m$ of ten sensors equispaced around the circumference of the $0.5m$ diameter duct.

The results are presented in figure 6. Qualitatively the results agree well for the most part with some minor differences. However, the magnitudes do not agree. Further work will have to be performed to determine the correct monopole volume source magnitude. In addition, although not plotted, the reflected radial modes from the WEM data, are in some instances very large, in contrast to the modes decomposed from the analytical data which are correctly close to zero for the infinite duct case. It is thought that the reason for this is that the radiation condition which was inherited from a free field configuration is inappropriate for the duct.

5.2 Versatility of the Wave Expansion Method.

Figure 7 shows a simple example of how the WEM method may be used to study a complex duct shape. Although the results are not verified here, qualitatively they appear to be correct with the higher modes clearly seen to be cut-off leaving only plane wave modes when the Helmholtz number is reduced to below $kR = 1.83$ in figure 7(b).

A second interesting result is seen in figure 8, where the $A_m = A_3$ mode is excited below its cut-on frequency causing it to be evanescent. This response matches closely that of experimental set-ups where monopole sources are approximated with loudspeakers, demonstrating the methods potential as a substitute or support for empirical work.

6. Conclusions

In this paper, the propagation of sound from point sources in hard-walled ducts is modelled using a numerical wave-based approach, referred to as the wave expansion method. The results are compared to an analytical Green's function solution. The pressure fields are found to compare extremely well when either specific or all acoustic modes are excited. The numerical solution is found to be sensitive to the mesh density with diminishing returns to be gained with increasing density. An acoustic modal decomposition was performed on the data, in both cases, with good qualitative agreement found for the azimuthal and incident radial modes. However, the reflected modes are erroneously high. This is thought to be due to a badly defined radiation condition at the end of the duct. Also, the monopole source magnitudes will have to be more correctly calculated to improve the agreement in the modal magnitudes. The versatility of the numerical (WEM) solution is demonstrated by examining a duct geometry of varying duct diameter and by its ability to study evanescent waves.

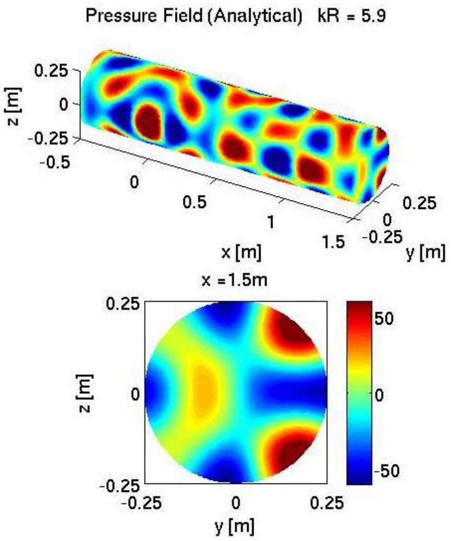

(a) Analytical solution for $kR = 5.9$.

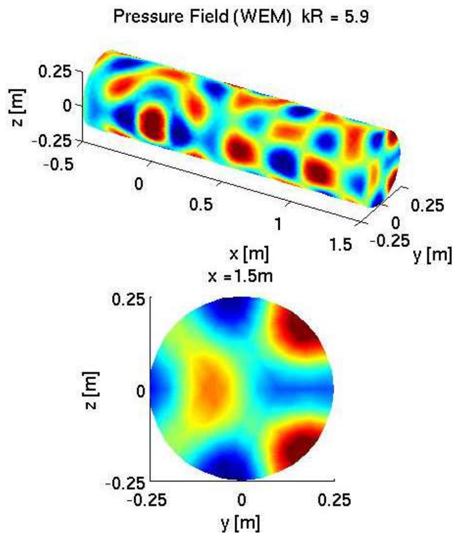

(b) Numerical (WEM) solution for $kR = 5.9$.

Figure 1. Pressure field in a duct excited by a single monopole source located on the duct surface at $(x, y, z) = (0, -0.25, 0)$

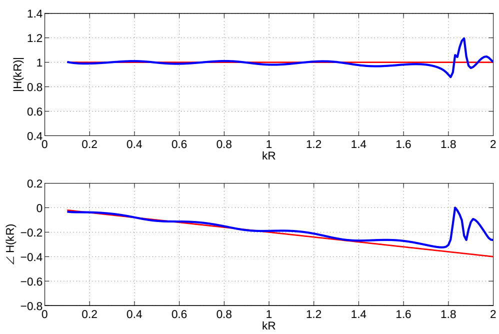

(a) Transfer function between two points on duct at same azimuthal angle separated axially by $0.05m$. Theory versus numerical results with mesh density of $0.26m$.

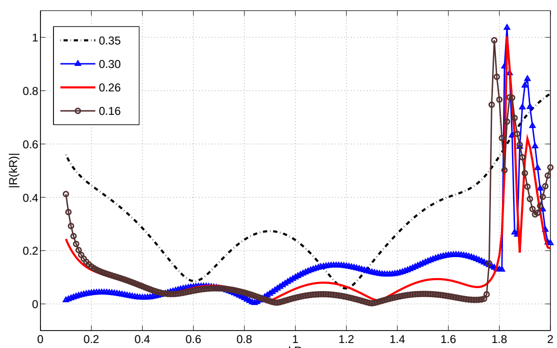

(b) Reflection coefficient as a function of mesh density.

Figure 2. Sensitivity of the WEM results to the mesh density.

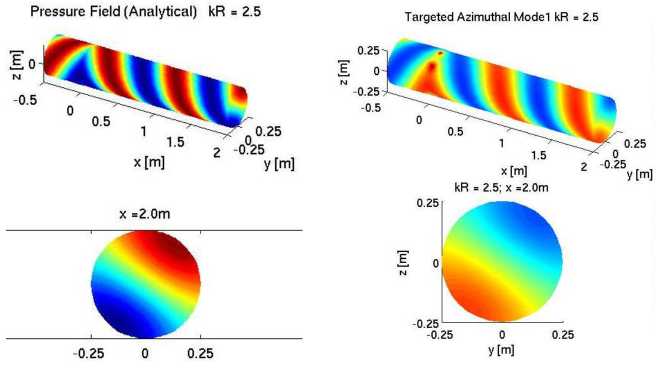

(a) Analytical solution for $kR = 2.5$.

(b) Numerical solution (WEM) for $kR = 2.5$.

Figure 3. Pressure field in a duct excited by eight monopole sources located equidistant around the duct surface at $x = 0$. Phases of monopoles adjusted to excite $A_m = A_1$.

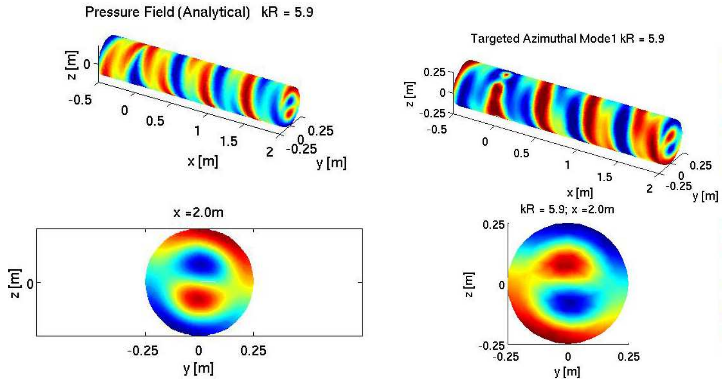

(a) Analytical solution for $kR = 5.9$.

(b) Numerical solution (WEM) for $kR = 5.9$.

Figure 4. Pressure field in a duct excited by eight monopole sources located equidistant around the duct surface at $x = 0$. Phases of monopoles adjusted to excite $A_m = A_1$.

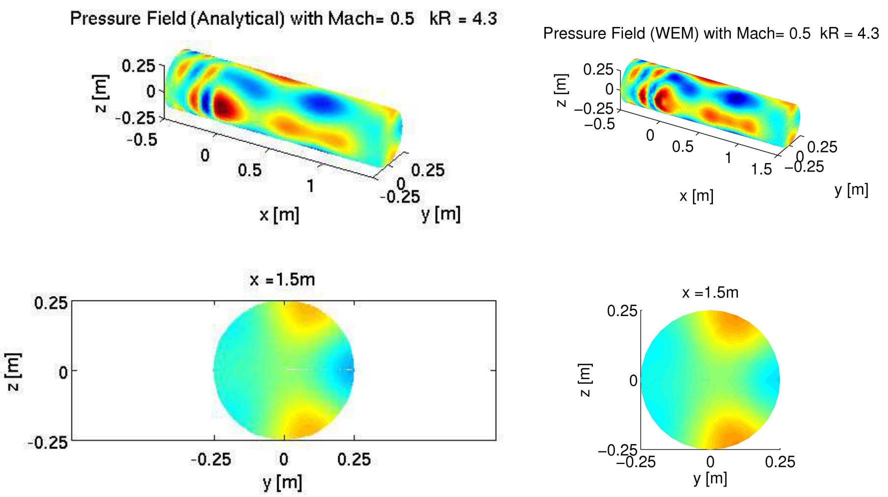

(a) Analytical solution for $kR = 4.3$.

(b) Numerical (WEM) solution for $kR = 4.3$.

Figure 5. Pressure field in a duct excited by a single monopole source located on the duct surface at $(x, y, z) = (0, -0.25, 0)$. Mean flow of Mach No.=0.5.

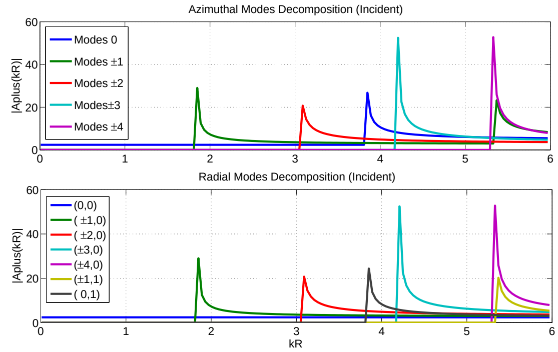

(a) Modal decomposition using analytical data.

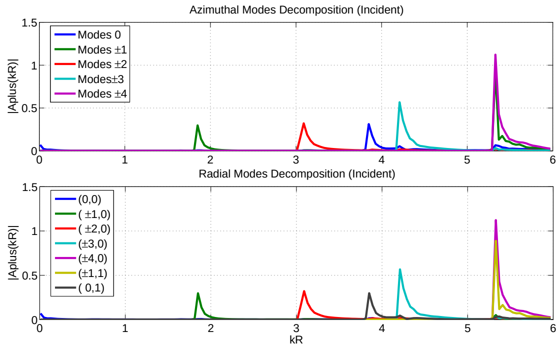

(b) Modal decomposition using numerical (WEM) data.

Figure 6. Azimuthal and radial (incident) modal decomposition in the duct excited by a monopole source.

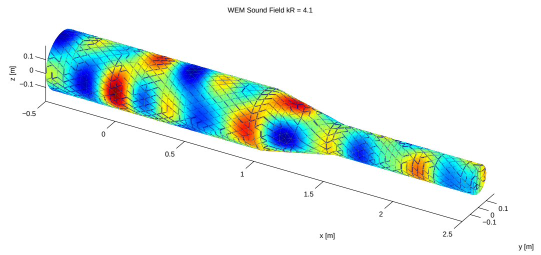

(a) $kR = 4.1$ for larger diameter reducing to $kR = 2.05$ for the smaller diameter.

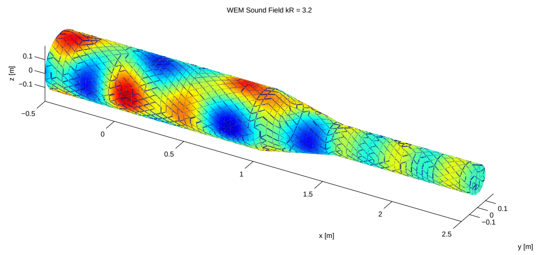

(b) $kR = 3.2$ for larger diameter reducing to $kR = 1.6$ for the smaller diameter.

Figure 7. Pressure field in a cylindrical duct of non-constant diameter, excited by a single monopole source. Numerical (WEM) solution.

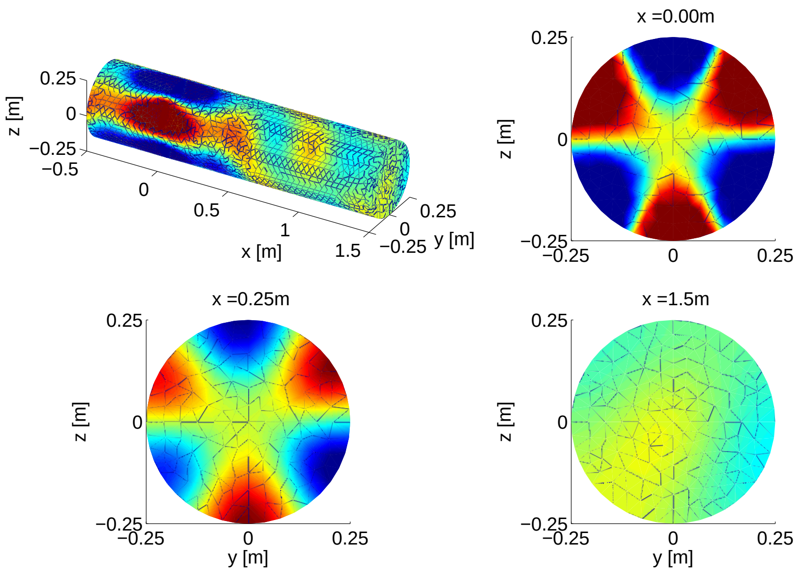

Figure 8. Numerical (WEM) solution for the sound field in a circular duct excited by eight monopole point sources. The target mode is $A_m = A_3$ but is excited below its cut-on frequency. The cross-sectional pressure field is calculated for three different axial locations.

REFERENCES

[1] J. E. Caruthers, R. C. Engels, and G. K. Ravinprakash. A wave expansion computational method for discrete frequency acoustics within inhomogeneous flows. In *AIAA/CEAS 2nd Aeroacoustics Conference*, State College, Pennsylvania, USA, 1996. AIAA-1996-1684.

[2] L. Barrera Rolla and H.J. Rice. A forward-advancing wave expansion method for numerical solution of large-scale sound propagation problems. *Journal of Sound and Vibration*, 296(1-2):406–415, 2006.

[3] P. Mungur and G. M. L. Gladwell. Acoustic wave propagation in a sheared fluid contained in a duct. *Journal of Sound and Vibration*, 9:28–48, 1969.

[4] M. L. Munjal. *Acoustics of Ducts and Mufflers*. John Wiley and Sons, 1987.

[5] L. E. Kinsler, A. R. Frey, A. B. Coppens, and J. V. Sanders. *Fundamentals of Acoustics*. John Wiley and Sons, fourth edition, 2000.

[6] G. Ruiz. *Numerical vibro/acoustic analysis at higher frequencies*. PhD thesis, University of Dublin, Trinity College, 2002.

[7] M. E. Goldstein. *Aeroacoustics*. McGraw-Hill International Book, 1976.

[8] J. Y. Chung and D. A. Blaser. Transfer function method of measuring in-duct acoustic properties. i. theory. *J. Acoust. Soc. Am.*, 68(3):907–913, 1980.

[9] Mats Åbom. Modal decomposition in ducts based on transfer function measurements between microphone pairs. Technical Report Report TRITA-TAK-8702, Department of Technical Acoustics, Royal Institute of Technology, Stockholm, Sweden, 1987.

[10] G. J. Bennett. *Noise Source Identification For Ducted Fans*. PhD thesis, Trinity College Dublin, 2006.

[11] Gareth J. Bennett, Ciaran O'Reilly, Ulf Tapken, and John Fitzpatrick. Noise source location in turbomachinery using coherence based modal decomposition. In *15th AIAA /CEAS Aeroacoustics Conference*, number AIAA-2009-3367, Miami, Florida, May 11-13 2009.

[12] Lars Enghardt, Yanchang Zhang, and Wolfgang Neise. Experimental verification of a radial mode analysis technique using wall-flush mounted sensors. In *137th Meeting of the Acoustical Society of America*, Berlin, March 1999.

[13] U. Tapken and L. Enghardt. Optimization of sensor arrays for radial mode analysis in flow ducts. In *12th AIAA/CEAS Aeroacoustics Conference*, number AIAA-2006-2638, Cambridge, MA., May 08-10 2006.